Fermi National Accelerator Laboratory

FERMILAB-Pub-80/90-THY
November 1980

Understanding Inclusive $pp \to ph^{\pm}X$ Data with Parton Fragmentation and Structure Functions

ALEXANDER NG
Ames Laboratory-DOE and Department of Physics,
Iowa State University, Ames, Iowa 50011

K.E. LASSILA
Fermi National Accelerator Laboratory, Batavia, Illinois 60510
and
Ames Laboratory-DOE and Department of Physics
Iowa State University, Ames, Iowa 50011

and

U.P. SUKHATME
Department of Physics, University of Illinois-Chicago Circle
Chicago, Illinois 60680

ABSTRACT

A model incorporating measured parton fragmentation and structure functions is shown to be in striking agreement with recent inclusive CERN-ISR data on charged hadrons produced in $pp \to ph^{\pm}X$ in the same hemisphere as the leading proton. These hadrons have low transverse momentum and the momentum of the leading proton is measured. The model is a realization at the parton level of the dual topological unitarization scheme for hadron-hadron collisions. Our work supports the attractive idea of universality of jets in both low-p_T and "hard" processes.

Operated by Universities Research Association Inc. under contract with the United States Department of Energy

Many recent investigations[1-4] have shown that a parton framework provides a fruitful and simple way for quantitatively describing low transverse momentum (p_T) multiparticle production in hadron-hadron collisions. In particular, the parton approach[1] based on dual topological unitarization (DTU)[5] has proved remarkably successful in explaining the rapidity and energy dependence of single particle inclusive distributions produced in hadronic collisions and in making predictions for forthcoming $\bar{p}p$ annihilation experiments.[6] In this approach, the sole input ingredients are parton fragmentation and structure functions determined from data on "hard" processes. The model is fully specified and has no free parameters. The success of such a model in explaining available low-p_T data is a strong indication of the universality of parton fragmentation (jet production) in various elementary particle reactions, as might be expected from a picture of multiparticle production via the confinement mechanism in an elongated color tube stretched between separating color charges.[7]

Recently, new CERN-ISR results have been published for the reaction $pp \to ph^{\pm}X$ at $\sqrt{s} = 62$ GeV. These authors[8] give the inclusive distribution of charged hadrons produced in the same hemisphere as the leading proton, whose momentum fraction x_p is measured. Since the proton is explicitly detected, these measurements contain information about the effect of baryon number conservation in a pp collision. Thus, these data offer a new and deeper probe for testing the validity of a parton approach to low-p_T physics. The purpose of this article is to demonstrate that the DTU-based parton model[1] can successfully account for the new data of Ref. 8. Accordingly, we will first briefly review the model, and adapt it to the situation where the momentum of the leading proton is known.

Since the DTU scheme[5] advocates the dominance of topological simplicity at high energies, the Pomeron has a cylindrical topology. A unitarity cut gives intermediate states corresponding to multiparticle production on two chains as illustrated in Fig. 1. More explicitly, in parton language, the Pomeron corresponds to an interchange between quarks i_1 and i_2 with momentum fractions x_1 and x_2 of the incident colliding protons. The probability of this interchange is taken to be proportional to the valence quark structure functions in a proton. The interaction produces color separation; for pp scattering, two separating quark-diquark systems are produced as depicted in Fig. 1, and their subsequent fragmentation by the confinement mechanism results in multiparticle production.

It is now necessary to discuss how the fast diquark gets converted into the leading baryon. Two obvious possibilities come readily to mind, and they are shown in Fig. 2. In the first case (Fig. 2a), the diquark produces a baryon leaving behind an antiquark which will fragment further, whereas in the second case (Fig. 2b) the diquark produces a meson leaving behind another diquark with reduced momentum. It is easy to see via the dimensional counting rules that Fig. 2a will dominate when the baryon takes away a large fraction of the incident diquark momentum. Since the experimental measurements[8] are at $x_p \gtrsim 0.5$, in this paper we shall assume that only Fig. 2a is present.[9] This assumption has been implicitly incorporated into Fig. 1. Clearly, the diquark momentum fraction $1 - x_1$ must be larger than the fraction x_p of the baryon into which it fragments, i.e.,

$$0 \leq x_1 \leq 1 - x_p \quad . \tag{1}$$

At this stage, we can formulate the 2-chain model quantitatively for the reaction $pp \to ph^{\pm}X$. The overall rapidity distribution is given by superposing the rapidity distributions in the 2 chains labelled A and B in Fig. 1,

$$\frac{1}{\sigma}\frac{d\sigma}{dy}\Big|^{pp\to phX}(s,y,x_p) = \sum_{i_1 i_2}\int_0^{1-x_p} dx_1 \int_0^1 dx_2 \rho^{pp}_{i_1 i_2}(x_1,x_2,x_p)\left[\frac{dN^h_A}{dy}(y-\Delta_A, P_A, x_p) + \frac{dN^h_B}{dy}(y-\Delta_B, P_B)\right] \tag{2}$$

where,

$$\rho^{pp}_{i_1 i_2}(x_1,x_2,x_p) = v^p_{i_1}(x_1)v^p_{i_2}(x_2)\Big/\sum_{i_1 i_2}\int_0^{1-x_p} dx'_1 \int_0^1 dx'_2 v^p_{i_1}(x'_1)v^p_{i_2}(x'_2) \tag{3}$$

is the conditional probability for the occurrence of a pp interaction capable of producing a final state proton with momentum fraction x_p. $v^p_i(x)$ is the structure function for valence quark i in the proton. The limits on the integration over x_1 are restricted by Eq. (1). The summation on i_1, i_2 is over the flavors u, d of valence quarks in the proton. Note that the ends of chain A correspond to a diquark of momentum $(1-x_1)P$ and a quark of momentum $-x_2P$ where P is the momentum of the incident colliding protons, $s = 4P^2$. It is therefore easy to make a Lorentz transformation from the overall pp CM frame to the CM frame of chain A. The Lorentz boost β_A, and the corresponding quantity β_B for chain B are given by[10]

$$\beta_A = \frac{(1-x_1)-x_2}{(1-x_1)+x_2} \quad , \quad \beta_B = \frac{x_1-(1-x_2)}{x_1+(1-x_2)} \quad . \tag{4}$$

In Eq. (2), the quantity P_A (P_B) denotes the CM momentum in the CM frame of chain A (B) and Δ_A (Δ_B) is the rapidity shift necessary to go from the overall pp CM frame to the CM frame of chain A (B),

$$P_A = [(1-x_1)x_2]^{1/2}P \quad , \quad 2\Delta_A = \ln[(1-x_1)/x_2] \quad ,$$

$$P_B = [x_1(1-x_2)]^{1/2}P \quad , \quad 2\Delta_B = \ln[x_1/(1-x_2)] \quad . \tag{5}$$

The baryon formed in chain B is not detected in the experiment of Ref. 8. Thus, the rapidity distribution for hadron h from chain B comes from quark-diquark fragmentation.[1] Therefore,

$$\frac{dN_B^h}{dy}(y - \Delta_B, P_B) = \begin{cases} \bar{x}_B D_{q\to h}(x_B) \quad , \quad y \geq \Delta_B \\ \\ \bar{x}_B D_{qq\to h}(x_B) \quad , \quad y < \Delta_B \end{cases} \tag{6}$$

where,

$$x_B = |\mu \sinh (y - \Delta_B)/P_B| \quad , \quad \bar{x}_B = \sqrt{x_B{}^2 + \mu^2/P_B{}^2} \quad , \tag{7}$$

and $\mu = 0.33$ is the canonical value for the transverse mass of a hadron.

In chain A, the leading proton is detected. It has momentum $x_p P$ in the overall pp CM frame; this corresponds to a momentum $x_p P_A/(1 - x_1)$ in the CM frame of chain A [from Eq. (4)]. In this frame, the initial diquark with momentum P_A becomes the leading proton, and the leftover antiquark therefore has momentum

$$P_Q = P_A - x_p P_A/(1 - x_1) \quad . \tag{8}$$

Hence, the rapidity distribution for hadron h from chain A effectively corresponds to quark-antiquark fragmentation

$$\frac{dN_A^h}{dy}(y - \Delta_A, P_A, x_p) = \begin{cases} \bar{x}_Q D_{\bar{q}\to h}(x_Q) \quad , \quad y \geq \Delta_A \\ \\ \bar{x}_A D_{q\to h}(x_A) \quad , \quad y < \Delta_A \end{cases} \tag{9}$$

where,

$$x_A = |\mu \sinh(y - \Delta_A)/P_A| \quad , \quad \bar{x}_A = \sqrt{x_A{}^2 + \mu^2/P_A{}^2}$$

$$x_Q = |\mu \sinh(y - \Delta_A)/P_Q| \quad , \quad \bar{x}_Q = \sqrt{x_Q{}^2 + \mu^2/P_Q{}^2} \quad . \tag{10}$$

Equations (2) to (10) fully specify the DTU parton model for the case of pp collisions in which the leading proton is measured. However, in order to compare with the experimental results of Ref. 8, it is necessary to convert to their variable $x_R{}^*$ which is defined by

$$x_R{}^* = p/E_{HAD} \quad , \quad E_{HAD} = P(1 - x_p) \quad , \tag{11}$$

where p is the momentum of the detected h and E_{HAD} is the hadronic energy in the hemisphere of the measured proton (not including the proton energy). Therefore

$$x_R{}^* \simeq \frac{x}{1 - x_p} \tag{12}$$

and,

$$dy = \frac{dx}{\sqrt{x^2 + \frac{\mu^2}{P^2}}} = \frac{dx_R{}^*(1 - x_p)}{\sqrt{x_R{}^{*2}(1 - x_p)^2 + \frac{\mu^2}{P^2}}} \quad . \tag{13}$$

Equation (13) permits conversion from dN/dy computed in Eq. (2) to the experimentally given quantity $dN/dx_R{}^*$. Figures 3 and 4a, b, c show a comparison of data[8] with the predictions of the DTU parton model which contains no adjustable parameters. In making these predictions, standard previous determinations of the structure functions[11] and fragmentation functions[1] from "hard" processes were used. Clearly, there is striking agreement of the model with the data for various values of x_p; furthermore, the normalization is correctly reproduced. Note that the model (in Fig. 3) reproduces the "crossover" phenomenon seen in the dN/dx_R^* data.[8] At first sight this appears to suggest meaningful physics, but it is easy to check that such behavior is just an artifact caused by the variable x_R^*. (A plot of dN/dx vs. x shows no crossovers.) In fact, in the DTU parton model, the variable x_R^* is not natural—we have used it only for making contact with the data of Ref. 8.

We note that our DTU-based two chain model is different from the suggestion in Ref. 8 that e^+e^- annihilation data (which results from a single $q\bar{q}$ chain) looks like pp data when the effects of baryon number conservation are removed by detecting the leading protons. In our model the two chains have smaller CM energies and predict an energy dependence in agreement with the rising rapidity plateaus seen over the ISR energy range (see Ref. 1).

In summary, our work lends additional support to the DTU-based parton model by probing it under novel circumstances. It further strengthens our belief that low-p_T physics may well be simply described in parton language, and that the forward-backward low-p_T jets and the jets seen in hard processes have a common origin consisting of separating color charges and their fragmentation due to color confinement.

ACKNOWLEDGMENTS

Two of the authors, K.E.L., and U.P.S., would like to thank the theory group and C. Quigg at Fermilab for the hospitality extended to them during the course of this work. One of the authors would like to thank Dr. Jean Lassila for encouragement.

REFERENCES AND FOOTNOTES

[1] A. Capella, U. Sukhatme and J. Tran Thanh Van, Zeit. Phys. C3, 329 (1980); A. Capella, U. Sukhatme, C.-I. Tan and J. Tran Thanh Van, Phys. Lett. 81B, 68 (1979).

[2] H. Minakata, Phys. Rev. D20, 1656 (1979); G. Cohen-Tannoudji et al., Phys. Rev. D21, 2699 (1980); B. Andersson, G. Gustafson and C. Peterson, Phys. Lett. 69B, 221 (1977) and 71, 337 (1977); S. Brodsky and J. Gunion, Phys. Rev. D17, 848 (1978); G. Cohen-Tannoudji, F. Hayot, and R. Peschanski, ibid., 17, 2930 (1978); and G. Cohen-Tannoudji, A. El Hassouni, J. Kalinowski, and R. Peschanski, ibid., 19, 3397 (1979).

[3] L. Van Hove and S. Pokorski, Nucl. Phys. B86, 243 (1975); W. Ochs, Nucl. Phys. B118, 397 (1977); K. Das and R. Hwa, Phys. Lett. 68B, 549 (1977); R. Hwa and R. Roberts, Zeit. Phys. C1, 81 (1979); E. Takasugi et al., Phys. Rev. D20, 211 (1979).

[4] For a review, see U. Sukhatme, in Proc. XIV Rencontre de Moriond, 1979, edited by J. Tran Thanh Van.

[5] G. Veneziano, Nucl. Phys. B74, 365 (1974) and B117, 519 (1976); Chan Hong Mo et al., Nucl. Phys. B86, 479 (1975) and B92, 13 (1975); G. Chew and C. Rosenzweig, Nucl. Phys. B104, 290 (1976) and Phys. Rep. 41C, 263 (1978).

[6] U. Sukhatme, Phys. Rev. Letters 45, 5 (1980).

[7] A. Casher, J. Kogut, and L. Susskind, Phys. Rev. D10, 732 (1974); A. Casher, H. Neuberger and S. Nussinov, Tel Aviv preprint (1978) unpublished; C. Chiu and S. Nussinov, Phys. Rev. D20, 945 (1979).

[8] M. Basile et al., (CERN, Bologna, Frascati), Phys. Letters 92B, 367 (1980).

[9] A more complete recursive model for diquark fragmentation which takes both Figs. 2a and 2b into account with appropriate weights can be found in U. Sukhatme, K. Lassila and R. Orava, Fermilab preprint (in preparation).

[10]In Eqs. (4) and (5) corrections of order m_Q^2/s, with m_Q = quark mass have been neglected. These corrections are easy to compute, as shown in Ref. 1, and are small at high energies. The numerical work was done with accurate formulae, with m_Q = 0.33 GeV.

[11]R. Field and R. Feynman, Phys. Rev. D15, 2590 (1977).

FIGURE CAPTIONS

Fig. 1: Multiparticle production in pp collisions via the dominant Pomeron contribution consisting of two quark-diquark chains.

Fig. 2: Diagrams for diquark fragmentation. (a) Fragmentation of a diquark into a baryon and an antiquark. (b) Fragmentation of a diquark into a meson and another diquark.

Fig. 3: Calculated inclusive hadron distributions for $pp \rightarrow phX$ in the variable $x_R^* = x/(1 - x_p)$ for leading proton momentum fraction $x_p = 0.5$ (dot-dash curve), $x_p = 0.7$ (dashed curve), and $x_p = 0.8$ (solid curve) for produced hadron energies 15 GeV, 9 GeV, and 6 GeV, respectively, where x is the fraction of the longitudinal momentum carried off by hadron h.

Fig. 4: Model predictions for the $x_R^* = x/(1 - x_p)$ distributions for charged hadrons produced in the same hemisphere as the leading proton compared with experimental data (from Ref. 8) for various leading proton momentum fractions (x_p) and hadron energies (E_{HAD}): (a) E_{HAD} = 5 to 8 GeV, x_p = .84 to .74; (b) E_{HAD} = 8 to 11 GeV, x_p = 0.74 -0.64; (c) E_{HAD} = 14-16 GeV, x_p = 0.55 - 0.48.

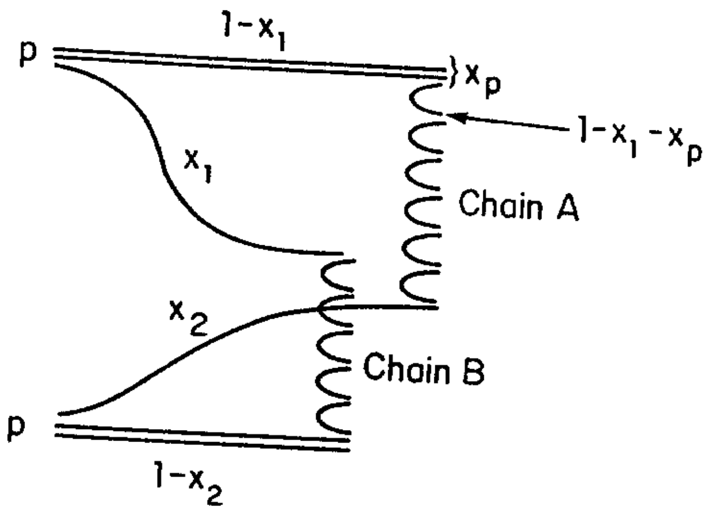

Fig. 1

Fig. 2

Fig 4a

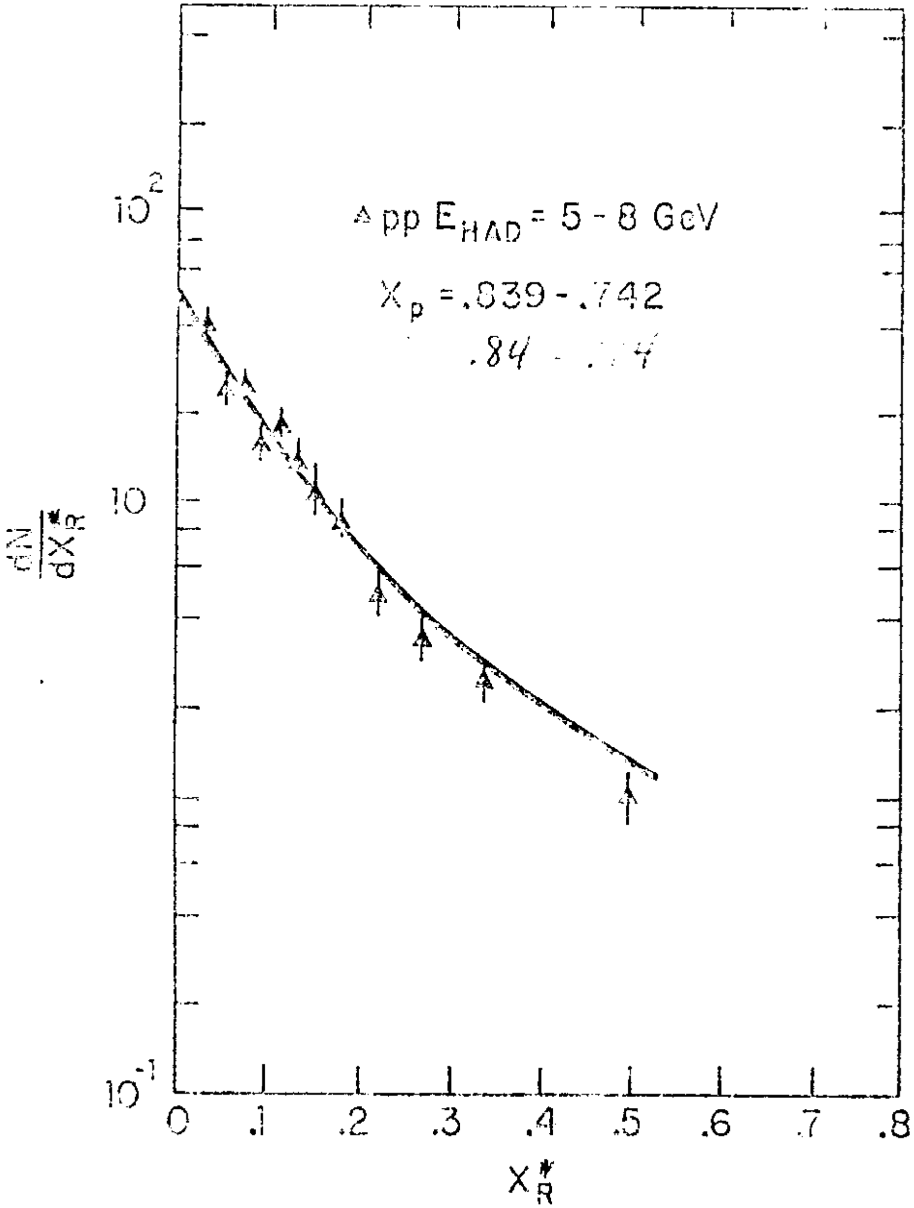

△ pp E_{HAD} = 5 - 8 GeV
X_p = .839 - .742
.84 - .74
10^2
10
10^{-1}
$\frac{dN}{dX_R^*}$
0
.1
.2
.3
.4
.5
.6
.7
.8
X_R^*

Fig 4b

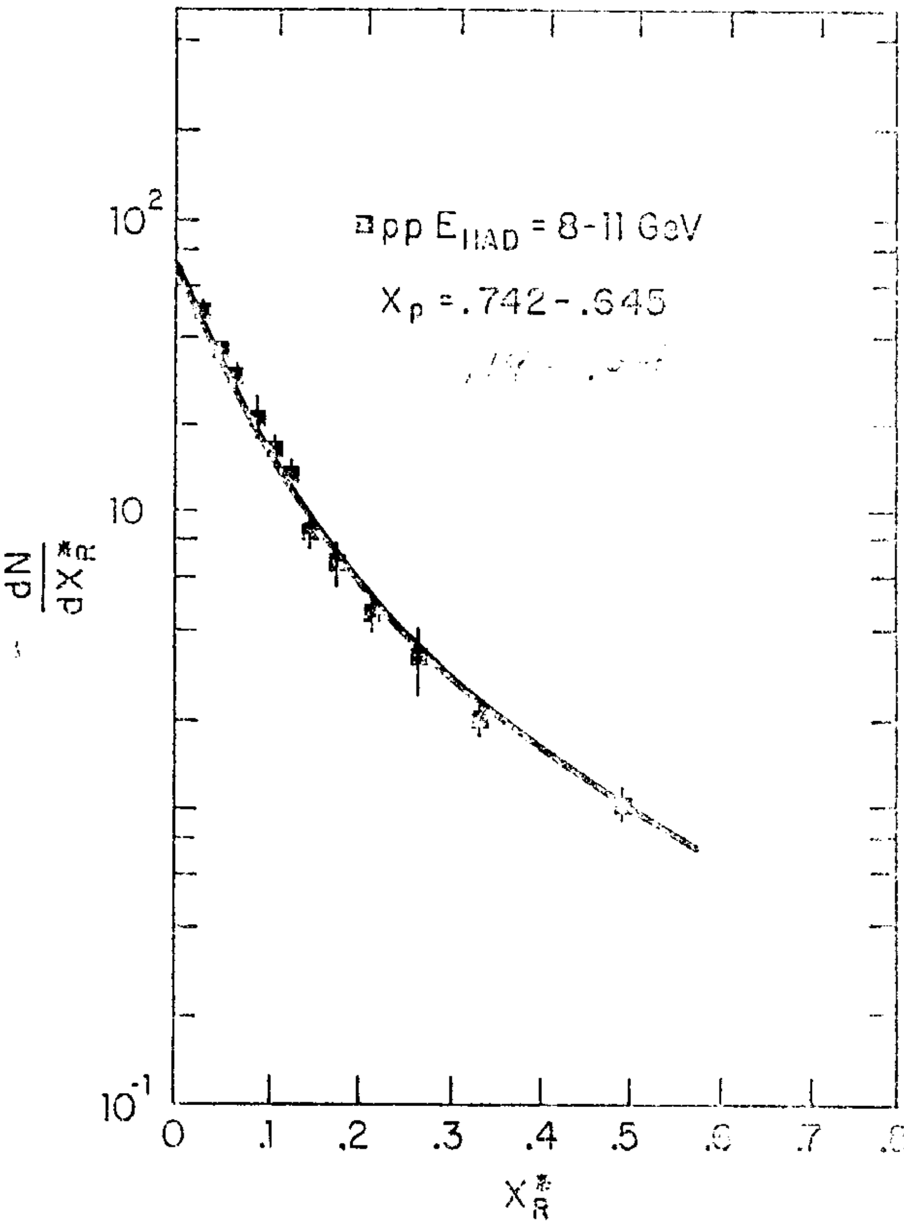

□ pp E_{HAD} = 8-11 GeV
X_p = .742 - .645
10^2
10
10^{-1}
$\frac{dN}{dX_R^*}$
0
.1
.2
.3
.4
.5
.6
.7
.8
X_R^*

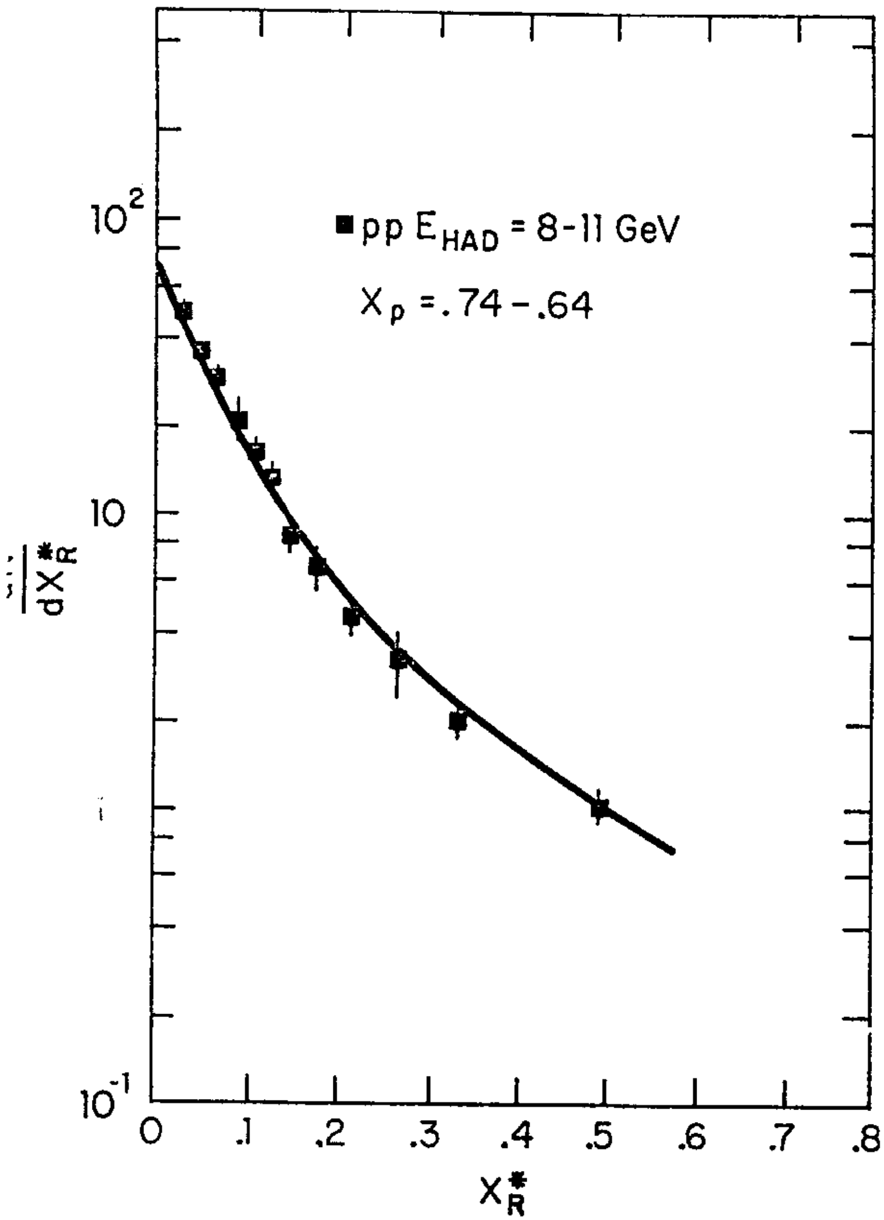

pp E_{HAD} = 8-11 GeV
X_p = .74 - .64
10^2
10
10^{-1}
0
.1
.2
.3
.4
.5
.6
.7
.8
X_R^*
$\frac{dN}{dX_R^*}$

Fig. 4b

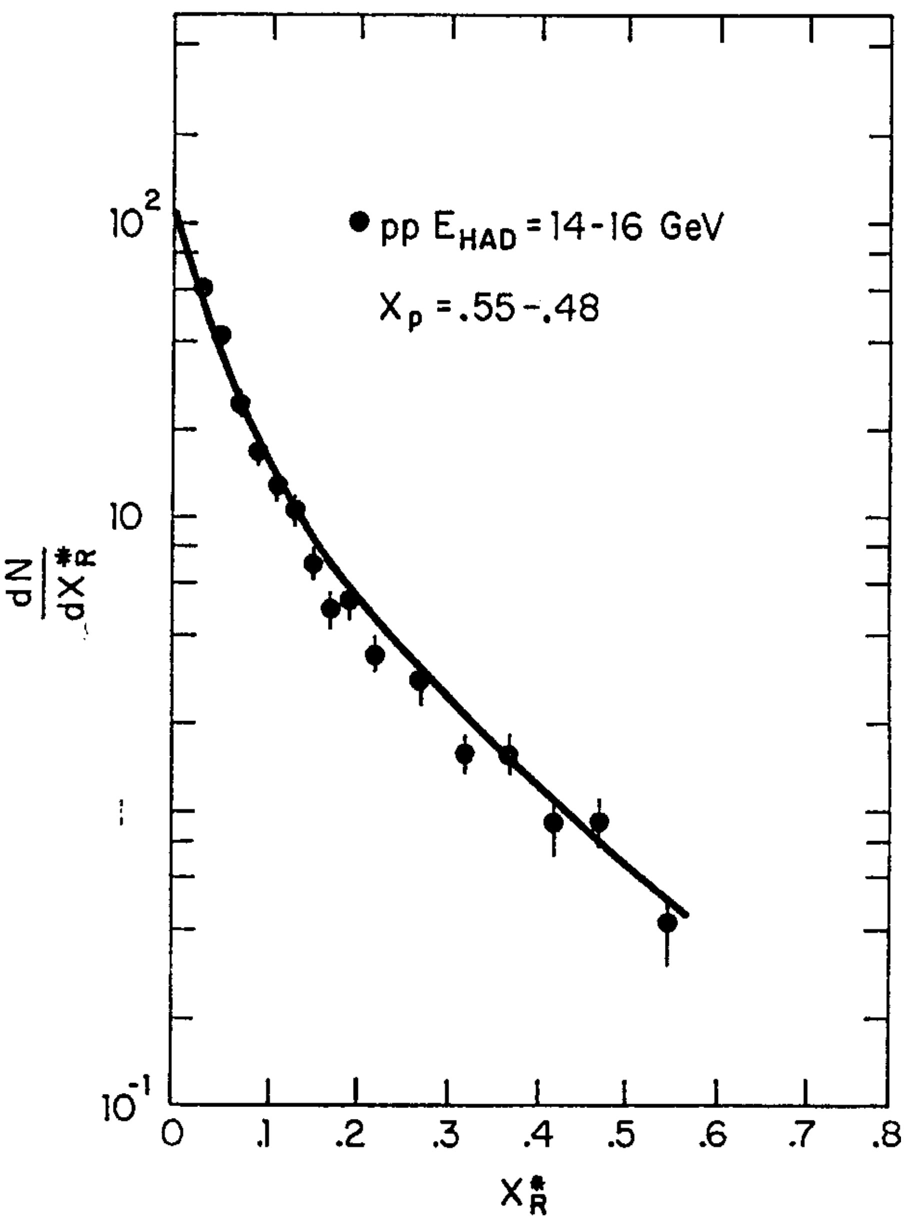

pp E_{HAD} = 14-16 GeV
X_p = .55 - .48
10^2
10
10^{-1}
0
.1
.2
.3
.4
.5
.6
.7
.8
X_R^*
$\frac{dN}{dX_R^*}$

Fig. 4c